Unique coupling of mono- and dioxygenase chemistries in a single active site promotes heme degradation

Toshitaka Matsui[a,1], Shusuke Nambu[a], Celia W. Goulding[b,c], Satoshi Takahashi[a], Hiroshi Fujii[d], and Masao Ikeda-Saito[a,1]

[a]Institute of Multidisciplinary Research for Advanced Materials, Tohoku University, Katahira, Aoba, Sendai 980-8577, Japan; [b]Department of Molecular Biology and Biochemistry, University of California, Irvine, CA 92697; [c]Department of Pharmaceutical Sciences, University of California, Irvine, CA 92697; and [d]Department of Chemistry, Graduate School of Humanities and Sciences, Nara Women's University, Kitauoyanishi, Nara 630-8506, Japan

Edited by Harry B. Gray, California Institute of Technology, Pasadena, CA, and approved February 26, 2016 (received for review November 26, 2015)

Bacterial pathogens must acquire host iron for survival and colonization. Because free iron is restricted in the host, numerous pathogens have evolved to overcome this limitation by using a family of monooxygenases that mediate the oxidative cleavage of heme into biliverdin, carbon monoxide, and iron. However, the etiological agent of tuberculosis, *Mycobacterium tuberculosis,* accomplishes this task without generating carbon monoxide, which potentially induces its latent state. Here we show that this unusual heme degradation reaction proceeds through sequential mono- and dioxygenation events within the single active center of MhuD, a mechanism unparalleled in enzyme catalysis. A key intermediate of the MhuD reaction is found to be *meso*-hydroxyheme, which reacts with O_2 at an unusual position to completely suppress its monooxygenation but to allow ring cleavage through dioxygenation. This mechanistic change, possibly due to heavy steric deformation of hydroxyheme, rationally explains the unique heme catabolites of MhuD. Coexistence of mechanistically distinct functions is a previously unidentified strategy to expand the physiological outcome of enzymes, and may be applied to engineer unique biocatalysts.

heme degradation | monooxygenation | dioxygenation | *Mycobacterium tuberculosis* | MhuD

Oxygenases catalyze substrate oxidation with incorporation of one or two oxygen atoms from O_2. The monooxygenation and dioxygenation reactions have little in common at the mechanistic levels and require different protein scaffolds, so that no enzyme is thought to catalyze the two distinct oxygenation modes in a single active site. Monooxygenases activate O_2 by using two electrons and two protons, which in total is equivalent to hydrogen peroxide (H_2O_2), and results in the release of one oxygen atom as a water molecule (Eq. **1**). Efficient proton and electron transfer machinery is equipped within the active sites of monooxygenases including cytochrome P450, where O_2 is reductively activated on the heme iron to form a high-valent oxo-species responsible for substrate monooxygenation (1, 2). In contrast, dioxygenases directly add two oxygen atoms of O_2 into substrates without consuming electrons and protons (Eq. **2**). Dioxygenase active sites are generally hydrophobic as observed for tryptophan and indoleamine 2,3-dioxygenases, where O_2 binds ferrous heme iron akin to cytochrome P450, but perform distinct chemistry (3–5). Prostaglandin-endoperoxide synthase, also known as cyclooxygenase (COX), is another type of dioxygenase where a nonactivated O_2 molecule binds to a fatty acid radical generated by initial hydrogen abstraction (6, 7). Whereas COX as well as linoleate diol synthase further convert the dioxygenated product with peroxidase or isomerase activity, respectively (6, 8), each dioxygenase has another active site designed for the latter reaction. Contrary to the conventional one active site, one reaction paradigm, here we report that MhuD, a heme-degrading enzyme from *Mycobacterium tuberculosis*, catalyzes a sequential monooxygenation and dioxygenation in its single active site.

$$RH + O_2 + 2e^- + 2H^+ \rightarrow ROH + H_2O, \quad [1]$$

$$R + O_2 \rightarrow R(O)_2. \quad [2]$$

Biological heme degradation proceeds through a unique self-oxidation mechanism where the substrate heme activates O_2 molecules. The canonical enzyme, heme oxygenase (HO), degrades heme into ferrous iron, carbon monoxide (CO), and biliverdin by three successive monooxygenation reactions (Fig. 1*A*) (9, 10). This mechanism, which passes through both hydroxyheme and verdoheme intermediates, has been considered the "gold standard" of heme degradation even for recently identified noncanonical HO-type enzymes (11–13). We have discovered, however, that MhuD cleaves the porphyrin ring without releasing CO, which is a clear indication of a distinct mechanism, without producing the verdoheme intermediate (14). MhuD products termed "mycobilins" (mycobilin-*a* and -*b* in Fig. 1*B*) retain the α-*meso* carbon atom at the cleavage site as a formyl group with an extra oxidation at either the β- or δ-*meso* position. MhuD has a single active site where heme is bound in an unusually distorted conformation, best described as ruffled (Fig. 1*C* and Fig. S1) (15, 16). The ruffling is expected to drastically modulate the heme-dependent O_2 activation to initiate this unique mechanism (14). Similar heme ruffling is observed for IsdG and IsdI (heme-degrading components of the iron regulated surface determinant system), MhuD homologs in *Staphylococcus aureus*, which liberate formaldehyde upon heme degradation instead of CO (17, 18).

Significance

Oxygenases are classified into two groups, mono- and dioxygenases, which, respectively, catalyze insertion of one and two oxygen atoms of O_2 into substrates. These two modes of oxygenation proceed through distinct reaction mechanisms and require totally different active site structures. For more than 60 years, oxygenase enzymes thus far have been found to catalyze either a mono- or dioxygenation reaction. This study has broken this paradigm as it clearly demonstrates that the heme-degrading enzyme from *Mycobacterium tuberculosis*, MhuD, catalyzes successive mono- and dioxygenation reactions within its single active site. This unprecedented bifunctionality of the single active center rationally explains the unique heme catabolites of MhuD, which have been proposed to meet the physiological demands of the pathogenic bacterium.

Author contributions: T.M. and M.I.-S. designed research; T.M., S.N., S.T., and M.I.-S. performed research; C.W.G. and H.F. contributed new reagents/analytic tools; and T.M. and M.I.-S. wrote the paper.

The authors declare no conflict of interest.

This article is a PNAS Direct Submission.

[1]To whom correspondence may be addressed. Email: matsui@tagen.tohoku.ac.jp or mis2@tagen.tohoku.ac.jp.

This article contains supporting information online at www.pnas.org/lookup/suppl/doi:10.1073/pnas.1523333113/-/DCSupplemental.

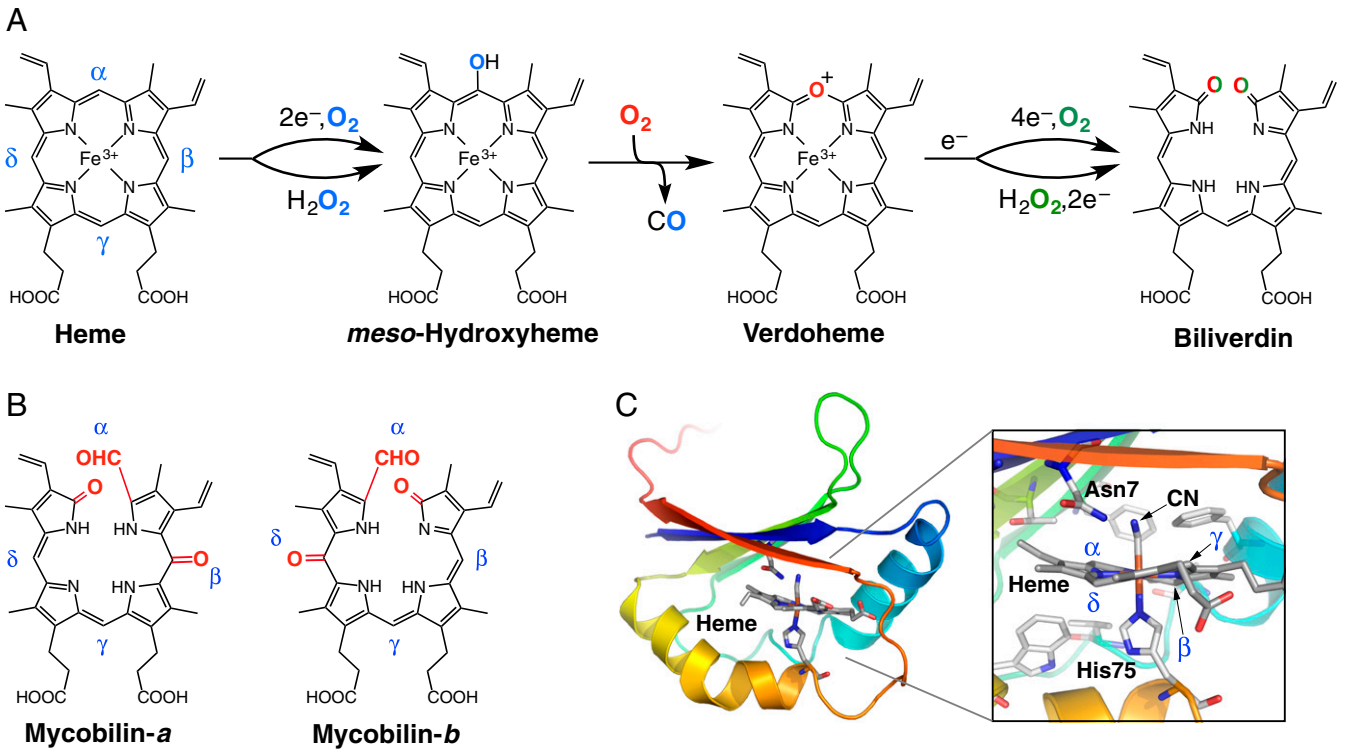

Fig. 1. HO- and MhuD-type heme degrading enzymes. (*A*) Heme degradation mechanism of canonical HO enzymes with alternative H_2O_2 pathways. (*B*) Structures of mycobilin isomers. (*C*) Crystal structure of cyanide-bound ferric heme-MhuD [Protein Data Bank (PDB) ID code 4NL5].

Results

First, we demonstrate that MhuD catalysis is initiated by reductive O_2 activation (O_2/e^-), suggesting HO-type self-monooxygenation. Reduction of ferric heme-MhuD in the presence of O_2 accumulates an intermediate with Soret and visible peaks at 407 and 560 nm, respectively (Fig. 2*A*). The same intermediate can be prepared by the reaction of ferrous heme-MhuD with O_2 (Fig. S2). Resonance Raman spectroscopy detects three $^{18}O_2$-sensitive signals, suggesting that this metastable intermediate is oxy-ferrous heme-MhuD (Fig. 2*B* and Table S1). Oxy-MhuD is further reduced to produce the mycobilin isomers in the presence of deferoxamine, a high-affinity iron chelator (Figs. 1*B* and 2*C*). We next find that H_2O_2 can substitute for the first O_2 activation (O_2/e^-) step, as expected for monooxygenation (19). The reaction of heme-MhuD and H_2O_2 in the absence of a reductant results in mycobilin formation with a similar isomer ratio (Fig. 2*C* and Fig. S3*A*). For H_2O_2-dependent mycobilin formation, there is a requirement for O_2 (Fig. S3*B*), suggesting the transient formation of *meso*-hydroxyheme, which is similar to its conversion in the HO second step that also strictly requires O_2 (Fig. 1*A*) (19, 20).

Formation of hydroxyheme from ferric heme-MhuD with H_2O_2 was examined under anaerobic conditions. The primary product exhibited its Soret peak at 402 nm with a visible peak at 573 nm (Fig. S4*A*). This absorption spectrum is distinct from that of MhuD complexed with chemically synthesized hydroxyheme (Fig. S4*C*). This species has no reactivity with O_2 and is likely to be ferryl heme-MhuD because addition of *p*-cresol, a typical substrate for one-electron oxidation, mostly regenerates the starting ferric heme complex (Fig. S4*A*). The dead-end ferryl heme may be generated by an uncoupling reaction of a putative hydroperoxy intermediate (FeOOH, Fig. S4*E*) (21). Because of this uncoupling pathway, heme-MhuD exhibits weak peroxidation activity of guaiacol (0.3 min^{-1} at pH 7.0), which is far lower than those of native peroxidases and is comparable to that of myoglobin (22). Reduction of ferryl heme, which is also achieved in the presence of deferoxamine (Fig. S4*B*), allows the regenerated ferric heme to cycle through another H_2O_2 reaction. If the H_2O_2 reaction affords a small amount of hydroxyheme via this pathway (Fig. S4*E*), its accumulation should become detectable upon multiple turnovers. In fact, a reaction of ferric heme-MhuD with a fourfold excess of H_2O_2 in the presence of deferoxamine results in the emergence of characteristic visible bands around 540 and 615 nm (Fig. S4*D*), indicating partial accumulation of hydroxyheme. The observed intermediate exhibits a similar reactivity as the hydroxyheme complex of MhuD as described below. Thus, the initial step of MhuD heme degradation is the inefficient conventional self-monooxygenation of heme to hydroxyheme through oxy-heme and possibly FeOOH-heme intermediates (Fig. 3) (20, 23, 24).

The hydroxyheme oxidation leading to ring cleavage has been reported to occur only at the hydroxylated site (on-site oxidation in Fig. 3) (25, 26). Despite the α-*meso* cleavage in both mycobilin isomers (Fig. 1*B*), α-hydroxyheme-MhuD does not afford mycobilin even in the presence of H_2O_2 and O_2 (Fig. 2*C* and Fig. S5*A*). Instead, β-hydroxyheme-MhuD produces mycobilin-*a* with the additional oxidation at the β-*meso* carbon atom, whereas mycobilin-*b* with the δ-*meso* oxidation is generated from δ-hydroxyheme-MhuD (Figs. 1*B* and 2*C*). β-Hydroxyheme-MhuD immediately exhibits a significant decrease in Soret absorbance and concomitant increase around 700 nm upon H_2O_2/O_2 addition, and this intermediate termed "X" is further converted into mycobilin by deferoxamine (Fig. 2*D*). These results indicate different reaction sites for primary hydroxylation (β- or δ-*meso* carbon atom) followed by oxidative ring cleavage at the α-*meso* position. The unusual "remote-site oxidation" in MhuD gives a rationale for the lack of CO produced because the conventional "on-site oxidation" would be a prerequisite to extrude the vicinal C–O moiety as CO (Fig. 3).

Quantitative analysis of the hydroxyheme conversion reveals that O_2 and deferoxamine, but not H_2O_2, are required to yield

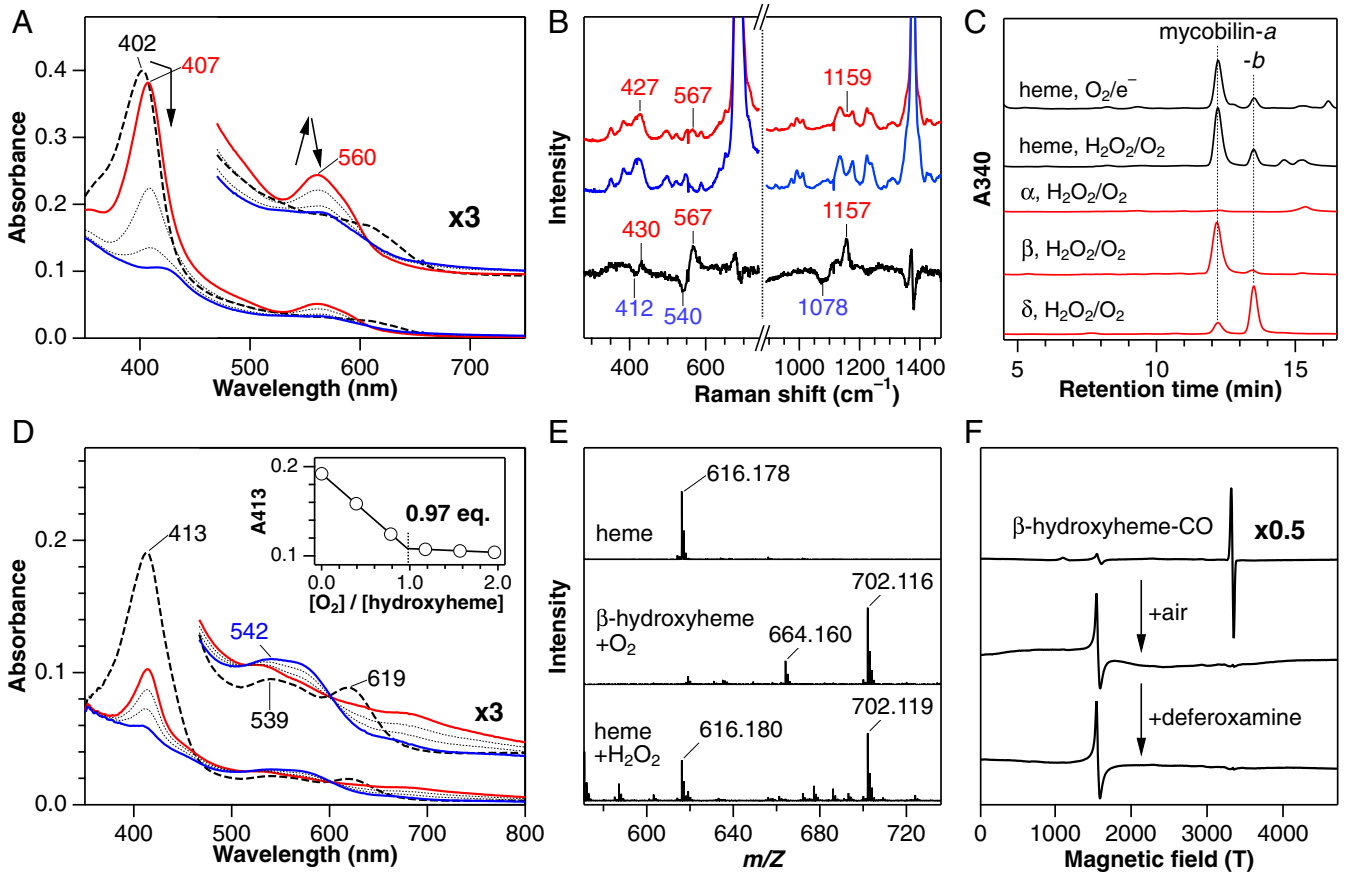

Fig. 2. Heme degradation by MhuD. (*A*) Absorption spectral change for reduction of ferric heme-MhuD (dashed) by sodium ascorbate in the presence of O_2 and deferoxamine at pH 6.0 and 37 °C. Spectra were recorded at 2 (red), 10 and 20 (dotted), and 30 min (blue) after the ascorbate addition. (*B*) Resonance Raman spectra of ferrous oxy-MhuD at pH 7.0 obtained with $^{16}O_2$ (red), $^{18}O_2$ (blue), and their difference (black). (*C*) HPLC chromatograms for degradation products of heme (black) and indicated isomers of *meso*-hydroxyheme (red) in the O_2/e^-- or H_2O_2-dependent reactions. (*D*) Absorption spectral change of β-hydroxyheme-MhuD (dashed) in conversion to mycobilin at pH 7.0 and 20 °C. Spectra were recorded at 1 (red), 6, and 15 (dotted), and 40 min (blue) after addition of H_2O_2/O_2 in the presence of deferoxamine. (*Inset*) Absorbance change at 413 nm upon titration with air-saturated buffer. (*E*) ESI-MS spectra of heme-MhuD (*Top*) and the intermediate X prepared by adding O_2 to β-hydroxyheme-MhuD under N_2 (*Middle*) or H_2O_2 to heme-MhuD under air (*Bottom*). (*F*) EPR spectra of CO-bound β-hydroxyheme-MhuD (*Top*) and its reaction products with O_2 (*Middle*) and with O_2/deferoxamine (*Bottom*) at 10 K.

mycobilin (Table S2). Titration experiments indicate that one molar equivalent of O_2 converts β-hydroxyheme-MhuD to X (Fig. 2*D*). The mycobilin formation from β-hydroxyheme also requires an equimolar amount of O_2 (Table S2). Electrospray ionization-mass spectrometry (ESI-MS) analysis of X shows positive-ion signals at 664.160 and 702.116 (Fig. 2*E*), which, respectively, correspond to H^+ and K^+ adducts of $[FeC_{34}H_{31}N_4O_7]$ (calculated: 664.162 and 702.118). The same K^+ adduct of X is also detected in the reaction of *heme*-MhuD with H_2O_2 in the presence of O_2 (Fig. 2*E*). The formula of X suggests addition of two oxygen atoms into β-hydroxyheme. The $^{18}O_2$-labeling experiments on X results in a mass increase by 4 (Fig. S6*A*), further corroborating the incorporation of two oxygen atoms. The two β-hydroxyheme incorporated oxygen atoms originate from the same O_2 molecule, because no isotope scrambling is observed for X produced with a mixture of $^{16}O_2$ and $^{18}O_2$ (Fig. S6*A*). Very similar results are obtained for δ-hydroxyheme-MhuD (Figs. S5*B* and S6*B* and Table S2). These findings unambiguously indicate incorporation of two oxygen atoms from one O_2 molecule; i.e., dioxygenation of hydroxyheme.

The hydroxyheme dioxygenation is also supported by following the $^{18}O_2$ labeling through to the mycobilin products. Optimization of the reaction and analysis conditions is required due to the problematic exchange of the formyl oxygen with water over a longer reaction time of 30 min for mycobilin instead of a few seconds for X. Once optimized, we detect a significant amount of doubly labeled mycobilin in the $^{18}O_2$ reactions of β- and δ-hydroxyheme-MhuD (Fig. S7 *A* and *B*). Moreover, MS analyses of these ^{18}O-labeling experiments initiated from *heme*-MhuD are consistent with the sequential mono/dioxygenation mechanism. In the reductive O_2 activation, the mycobilin isomers appear to accommodate three oxygen atoms from O_2, one of which is exchangeable with water (Fig. S7 *C* and *D*). In the H_2O_2/O_2 reaction, one nonexchangeable oxygen is inserted from H_2O_2 into X and mycobilin (Figs. S6*C* and S7 *E* and *F*), identifying the initial H_2O_2 reaction as a monooxygenation process. At the latter stage, insertion of two oxygen atoms from O_2 appears to occur, one of which is again exchangeable with water (Fig. S7 *E* and *F*).

The high reactivity of ferric hydroxyheme with O_2 is attributed to its resonance with a ferrous porphyrin radical form (Fig. 3). As reported for HO (23, 24), "ferric" hydroxyheme-MhuD binds CO, a typical ferrous iron ligand, to exhibit an intense radical EPR signal (Fig. 2*F*). CO binding does not interfere with the hydroxyheme-MhuD reaction (Fig. S5*C*), suggesting O_2 binding to the heme periphery rather than on the iron (23). Similar radical addition of O_2 is observed for dioxygenases including COX and lipoxygenase (6, 7), both of which initially oxidize their substrate by one electron. Lipoxygenase as well as MhuD

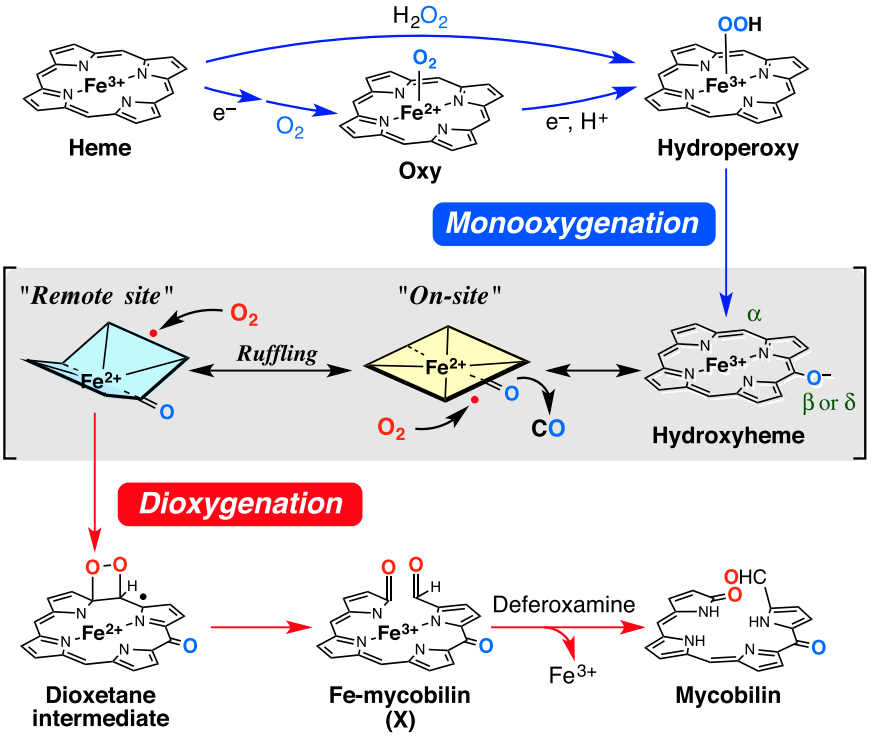

Fig. 3. Heme degradation mechanism of MhuD.

uses a ferric iron to generate the substrate radical, whereas the intermolecular electron transfer is not required for MhuD owing to the intrinsic radical properties of hydroxyheme. To produce mycobilin, O_2 is destined to covalently bond with both the *meso* and pyrrole carbon atoms, probably to yield a dioxetane intermediate (Fig. 3) (27). Following O–O bond cleavage, a ferric–mycobilin complex would be produced, whose iron is finally removed by deferoxamine. Stepwise dioxygenation-like Criegee rearrangement is improbable because it would require temporary holding of one oxygen atom by iron (27, 28).

The mass signals of the intermediate X (Fig. 2*E*) are consistent both with the ferric–mycobilin and dioxetane forms having the same mass number (the open and closed ring structures, Fig. 3). Nevertheless, the intermediate X prepared either from β- or δ-hydroxyheme-MhuD with $^{18}O_2$ shows a mass decrease by 2 after incubation under either N_2 or normal air (Fig. S6 *D* and *E*, respectively). This finding clearly indicates exchange of one oxygen atom with water but not with O_2, strongly suggesting the ferric–mycobilin structure for X. This assignment is consistent with the fact that deferoxamine facilitates mycobilin formation from X presumably by capturing iron released from the open ring intermediate (Fig. 2*D*). Moreover, an EPR signal of X observed at $g \sim 4.3$ (Fig. 2*F*) suggests a highly rhombic environment for iron, as observed for ferric–biliverdin complexes of HO (29) and myoglobin (26). One may speculate that the rhombic signal arises from free iron released upon unexpected decomposition of X during the EPR measurement, especially because the spectra of X and the ferric iron–deferoxamine complex closely resemble each other (Fig. 2*F*). However, the EPR sample of X exhibited a distinct color change to purple, characteristic of mycobilin, upon addition of deferoxamine, inferring that the majority of iron in the EPR sample of X is still complexed with the tetrapyrrole ligand.

Discussion

Our study identifies MhuD as the first enzyme, to our knowledge, that performs both monooxygenation and dioxygenation in a single active site (Fig. 3). This enzyme appears to be designed primarily for dioxygenation with minimum adaptation to monooxygenation. Inefficiency of monooxygenation is evident both in the H_2O_2- (Fig. S4) and O_2/e^- reactions of MhuD (14), probably due to its predominantly hydrophobic heme environment lacking a proton-donating candidate to control the reactive FeOOH intermediate (16, 30). Such a structural defect for monooxygenation can be a trade-off for an efficient dioxygenation reaction. The hydroxyheme intermediate is dioxygenated with a stoichiometric amount of O_2 (Fig. 2*D*) while almost completely suppressing the monooxygenation pathway as evident from a negligible formation of CO (14). The high hydrophobicity of the dioxygenase active sites is expected to increase O_2 affinity and suppress undesired reactions through nonregulated protonation, although its exact roles are yet to be clarified. Moreover, in the MhuD active site, the hydrophobic residues forming noncovalent bonds with heme might also be critical for its ruffling (Fig. S1*C*).

The most important determinant to enable MhuD hydroxyheme dioxygenation should be the remote-site oxidation, i.e., the regiospecific oxygenation of the nonhydroxylated *meso*-carbon (Fig. 3). Because all of the three successive oxygenations by canonical HO take place at the same position to cleave the heme ring, the initial hydroxylation by MhuD was believed to occur on the α-*meso* carbon atom. In this study, however, MhuD is shown to primarily hydroxylate the β- or δ-*meso* carbon atoms, and then to dioxygenate the α-*meso* position. The β/δ preference in the first hydroxylation is not due to a result of an approximation effect accompanied by the heme ruffling. The β- and δ-*meso* carbon atoms in MhuD deviate from the heme plane toward the heme proximal side (Fig. 1*C*), while the reactive FeOOH species should be generated in the heme distal pocket. It is more likely that a hydrogen bond interaction directs the terminal OH moiety of FeOOH to Asn7, which is the only polar residue within the MhuD active site located above the δ-*meso* carbon atom. Normally, heme can be rotated 180° along the α-γ axis to position Asn7 in close proximity of the β-*meso* carbon atom as well.

In the following dioxygenation, O_2 is not activated on the central iron but is expected to directly attack the porphyrin ring. This mechanistic difference of the first and second oxygenation allows exhibition of their different regioselectivity even though the normal on-site oxidation of hydroxyheme results in the same regioselectivity. Studies on COX and lipoxygenase have concluded that their regioselectivity for the radical addition of O_2 is controlled cooperatively by several factors including steric shielding and radical localization (31). Because the β-, γ-, and δ-*meso* heme carbons appear to be accessible (Fig. S1 *D* and *E*), a major requirement in MhuD product formation seems to be radical localization on the α-*meso* carbon (Fig. 3), which may be induced by ruffling of hydroxyheme. Further, ruffling of heme has been suggested to promote the initial monooxygenation by changing its electronic structure (16, 32). Thus, the unique substrate deformation appears to enhance two different modes of oxygenation at different stages of catalysis to achieve the unprecedented dual function of MhuD. This further suggests that the MhuD homologs in *S. aureus*, IsdG and IsdI, also perform both modes of oxygenation due to similarities in their single hydrophobic active sites that bind highly ruffled heme (17, 33). Cramming two mechanistically distinct functions into one enzyme active site must have required high evolutionary pressure to yield a structure that promotes this unique bifunctional reaction. Unraveling this "cramming" method could provide a blueprint for the biomimetic design of artificial enzymes with extended functions.

Materials and Methods

Materials. A stable isotope labeled oxygen gas ($^{18}O_2$) was obtained from Taiyo Nippon Sanso. $H_2{}^{18}O_2$ and hydroxyheme were synthesized as reported earlier (23, 34). The ^{18}O content of the $H_2{}^{18}O_2$ solution was estimated to be ∼80% by analyzing the $H_2{}^{18}O_2$-dependent biliverdin formation by rat HO-1. Concentration of H_2O_2 was determined by horseradish peroxidase-assisted iodide oxidation using ε_{353} (triiodide) = 2.6×10^4 $M^{-1}{\cdot}cm^{-1}$ (35). Other chemicals obtained from Wako and Aldrich were used without further purification. Catalase and superoxide dismutase were purchased from Sigma. The MhuD protein was purified as a heme-free form as reported earlier (14). Preparation of a heme complex of rat HO-1 was performed according to a method described previously (36).

Reconstitution of MhuD with Heme or Hydroxyheme. MhuD can bind up to two molecules of heme in its catalytic center while the active form is the 1:1 complex (Fig. S1 *A* and *B*) (15). The monoheme–MhuD complex was selectively prepared by incubating the purified protein in 20 mM Tris·HCl, pH 8.0 containing 10 mM NaCl with 1.0 molar equivalent of hemin at 4 °C for 12 h. The crude complex was loaded on an anion exchange column (DE52, Whatman) equilibrated with 0.1 M potassium phosphate, pH 7.0 and the monoheme complex was eluted with the same buffer containing 350 mM NaCl. Anaerobic reconstitution of heme-free MhuD with the hydroxyheme isomers was performed as reported for rat HO-1 (23). Hydroxyheme dissolved in 0.1 M KOH was added to approximately twofold excess of heme-free MhuD in 0.1 M potassium phosphate, pH 7.0 at 4 °C for 8 h in an anaerobic glove box (MBraun, UNIlab). The hydroxyheme complex was purified by gel filtration chromatography (Sephadex G-25, GE Healthcare). Absorption coefficients of β- and δ-hydroxyheme-MhuD in 0.1 M potassium phosphate, pH 7.0 at 20 °C were determined by anaerobic titration with sodium dithionite to be 80 and 65 $mM^{-1}{\cdot}cm^{-1}$ at 413 and 410 nm, respectively. Alternate titrations of hydroxyheme-MhuD and horse myoglobin were performed to standardize the dithionite solution. UV-vis absorption spectra were recorded on Agilent 8453 and Shimadzu UV1500 diode array spectrophotometers for reactions in the presence and absence of O_2, respectively.

Heme Degradation. Heme degradation by reductive O_2 activation was performed in 0.1 M Mes, pH 6.0 at 37 °C containing ∼4 μM heme-MhuD, 25 mM sodium ascorbate, 2.5 mM deferoxamine, 50 U/mL superoxide dismutase, and 4.5 kU/mL catalase. Oxy-MhuD accumulated in the weakly acidic condition. Heme degradation with H_2O_2 was typically examined in 0.1 M potassium phosphate, pH 7.0 at 20 °C with 100 μM H_2O_2 and 2.5 mM deferoxamine. All of the reactions under anaerobic condition, reactions with $^{18}O_2$, $^{16}O_2/^{18}O_2$ and controlled amounts of O_2, and reactions of hydroxyheme-MhuD, were performed in the anaerobic glove box. Reactions of α- and β-hydroxyheme were examined in 0.1 M potassium phosphate, pH 7.0 at 20 °C while the temperature was increased to 30 °C for the less reactive δ-isomer. O_2 was injected with a gas-tight syringe or added as air-saturated water. Absorption spectral changes during the reactions were monitored by the diode array spectrophotometers without UV light illumination to avoid severe photoreaction. For quantitative analysis of mycobilin, 5 μM propiophenone was added as an internal standard after completion of the reaction. Solid-phase extraction of the reaction products was performed with Supelclean LC-18 columns (100 mg, Supelco). The sample bound to the column was washed with 1 mL 20% methanol/80% water (vol/vol) and eluted with 150 μL methanol. The effluents were analyzed on a Shimadzu LC-10 HPLC system equipped with a Tosoh ODS-80T_m reverse-phase column (4.6 × 150 mm) using a linear gradient from 45% 0.1 M ammonium acetate/55% methanol (vol/vol) to 70% methanol (vol/vol) over 15 min at a flow rate of 1 mL/min. The eluate was monitored using a Shimadzu photodiode array detector (SPD-M20A).

Resonance Raman Spectra. Resonance Raman spectra were obtained by excitation using the 405-nm line of a solid-state laser (Omicron-Laserage Laserprodukte GmbH, Bluephoton LDM405.120.CWA.L.WS). The scattered light at 90° was dispersed with a single polychrometer (Princeton Instruments, Acton SpectraPro SP-2500) and detected by a cooled CCD detector (Roper Scientific, CCD-1340/400-EM). The laser power on the sample was ∼20 mW with the accumulation time of 30 min. The sample cell was cooled by a cryostream of N_2 at ∼4 °C and rotated at 800 rpm. The Raman shifts were calibrated with indene. Oxy-ferrous heme-MhuD in 0.1 M potassium phosphate, pH 7.0 was prepared by adding either $^{16}O_2$ or $^{18}O_2$ to ferrous heme-MhuD just before the measurements. The ferrous heme-MhuD solution was prepared in the anaerobic glove box by reducing the ferric heme-MhuD with excess sodium dithionite, which was removed by gel filtration chromatography using a G-25 column.

Peroxidation Assay. Peroxidation activity of guaiacol was measured with 2 μM heme-MhuD, 100 μM H_2O_2, and 1.0 mM guaiacol in 0.1 M potassium phosphate, pH 7.0 at 20 °C. Guaiacol oxidation was monitored at 470 nm by using ε_{470} = 26.6 $mM^{-1}{\cdot}cm^{-1}$ (37). The initial rate was calculated from the absorbance increase at 1 min after the H_2O_2 addition. Significant deactivation was observed for heme-MhuD probably due to simultaneous heme degradation.

EPR Spectra. EPR spectra were obtained at 10 K by a Bruker ELEXSYS E580 spectrometer in the continuous wave mode operating at 9.38 GHz with an incident microwave power of 0.2 mW and 5-G field modulation at 100 kHz. An Oxford liquid helium flow cryostat with a Mercury iTC temperature controller was used for cryogenic measurements. The microwave frequency was monitored by a frequency counter (Bruker SuperX-FT bridge), and the magnetic field was determined by a teslameter (Bruker ER 036TM). A 100 μM solution of β-hydroxyheme-MhuD in 0.1 M potassium phosphate, pH 7.0 was bubbled with 100 μL CO and sealed in an EPR tube. After data acquisition, air was introduced in the tube to prepare the intermediate X. Further reaction with deferoxamine was performed at 37 °C for 1 h. The mycobilin formation was confirmed by color change of the reaction solution to purple.

ESI-MS Analysis. ESI-MS spectra in positive ion mode were measured on a Bruker micrOTOF-Q-II mass spectrometer calibrated with sodium formate. Reaction intermediates of MhuD were analyzed by direct infusion at 5 μL/min with the following optimized settings: end plate offset, –500 V; capillary, –4,500 V; nebulizer gas, 0.4 bar; dry gas, 4.0 L/min; dry gas temperature, 180 °C; in-source collision induced dissociation, 140 eV. The mycobilin products were solid phase extracted as noted above with an extra wash step with 10 mL of 30% methanol/70% water/0.1% acetic acid (vol/vol) to remove deferoxamine. The concentrated samples were analyzed by LC-MS by using an Agilent 1260 HPLC system with higher nebulizer gas pressure (1.6 bar) and a dry gas flow rate (8.0 L/min). LC separation with an Agilent Extend-C18 reverse-phase column (2.1 × 150 mm) was performed using a linear gradient from 50% 10 mM ammonium acetate/50% methanol (vol/vol) to 70% methanol (vol/vol) over 15 min at a flow rate of 0.2 mL/min.

ACKNOWLEDGMENTS. We thank Dr. C. S. Raman for helpful comments. This work has been supported by Grants-in-Aid for Scientific Research (2412006 and 24350081 to M.I.-S.; 23550186, 25109504, 15K05555, and 15H00912 to T.M.) from Japan Society for the Promotion of Science and The Ministry of Education, Culture, Sports, Science and Technology (MEXT), Japan; by Strategic Alliance Project for the Creation of Nano-Materials, Nano-devices, and Nanosystems from MEXT, Japan; and by National Institutes of Health Grant AI081161 (to C.W.G.).

1. Denisov IG, Makris TM, Sligar SG, Schlichting I (2005) Structure and chemistry of cytochrome P450. *Chem Rev* 105(6):2253–2277.
2. Rittle J, Green MT (2010) Cytochrome P450 compound I: Capture, characterization, and C-H bond activation kinetics. *Science* 330(6006):933–937.
3. Sugimoto H, et al. (2006) Crystal structure of human indoleamine 2,3-dioxygenase: Catalytic mechanism of O_2 incorporation by a heme-containing dioxygenase. *Proc Natl Acad Sci USA* 103(8):2611–2616.
4. Forouhar F, et al. (2007) Molecular insights into substrate recognition and catalysis by tryptophan 2,3-dioxygenase. *Proc Natl Acad Sci USA* 104(2):473–478.
5. Millett ES, et al. (2012) Heme-containing dioxygenases involved in tryptophan oxidation. *Curr Opin Chem Biol* 16(1-2):60–66.
6. Rouzer CA, Marnett LJ (2003) Mechanism of free radical oxygenation of polyunsaturated fatty acids by cyclooxygenases. *Chem Rev* 103(6):2239–2304.
7. Tsai AL, Kulmacz RJ (2010) Prostaglandin H synthase: Resolved and unresolved mechanistic issues. *Arch Biochem Biophys* 493(1):103–124.
8. Su C, Sahlin M, Oliw EH (1998) A protein radical and ferryl intermediates are generated by linoleate diol synthase, a ferric hemeprotein with dioxygenase and hydroperoxide isomerase activities. *J Biol Chem* 273(33):20744–20751.
9. Ortiz de Montellano PR (1998) Heme oxygenase mechanism - Evidence for an electrophilic, ferric peroxide species. *Acc Chem Res* 31(9):543–549.
10. Matsui T, Unno M, Ikeda-Saito M (2010) Heme oxygenase reveals its strategy for catalyzing three successive oxygenation reactions. *Acc Chem Res* 43(2):240–247.
11. Suits MD, et al. (2005) Identification of an *Escherichia coli* O157:H7 heme oxygenase with tandem functional repeats. *Proc Natl Acad Sci USA* 102(47):16955–16960.
12. Wilks A, Burkhard KA (2007) Heme and virulence: How bacterial pathogens regulate, transport and utilize heme. *Nat Prod Rep* 24(3):511–522.
13. Guo Y, et al. (2008) Functional identification of HugZ, a heme oxygenase from *Helicobacter pylori*. *BMC Microbiol* 8:226.
14. Nambu S, Matsui T, Goulding CW, Takahashi S, Ikeda-Saito M (2013) A new way to degrade heme: The *Mycobacterium tuberculosis* enzyme MhuD catalyzes heme degradation without generating CO. *J Biol Chem* 288(14):10101–10109.
15. Chim N, Iniguez A, Nguyen TQ, Goulding CW (2010) Unusual diheme conformation of the heme-degrading protein from *Mycobacterium tuberculosis*. *J Mol Biol* 395(3):595–608.
16. Graves AB, et al. (2014) Crystallographic and spectroscopic insights into heme degradation by *Mycobacterium tuberculosis* MhuD. *Inorg Chem* 53(12):5931–5940.
17. Lee WC, Reniere ML, Skaar EP, Murphy ME (2008) Ruffling of metalloporphyrins bound to IsdG and IsdI, two heme-degrading enzymes in *Staphylococcus aureus*. *J Biol Chem* 283(45):30957–30963.
18. Matsui T, et al. (2013) Heme degradation by *Staphylococcus aureus* IsdG and IsdI liberates formaldehyde rather than carbon monoxide. *Biochemistry* 52(18):3025–3027.
19. Wilks A, Ortiz de Montellano PR (1993) Rat liver heme oxygenase. High level expression of a truncated soluble form and nature of the *meso*-hydroxylating species. *J Biol Chem* 268(30):22357–22362.
20. Matsui T, et al. (2005) O_2- and H_2O_2-dependent verdoheme degradation by heme oxygenase: Reaction mechanisms and potential physiological roles of the dual pathway degradation. *J Biol Chem* 280(44):36833–36840.
21. Matsui T, Furukawa M, Unno M, Tomita T, Ikeda-Saito M (2005) Roles of distal Asp in heme oxygenase from *Corynebacterium diphtheriae*, HmuO: A water-driven oxygen activation mechanism. *J Biol Chem* 280(4):2981–2989.
22. Sievers G, Rönnberg M (1978) Study of the pseudoperoxidatic activity of soybean leghemoglobin and sperm whale myoglobin. *Biochim Biophys Acta* 533(2):293–301.
23. Matera KM, et al. (1996) Oxygen and one reducing equivalent are both required for the conversion of α-hydroxyhemin to verdoheme in heme oxygenase. *J Biol Chem* 271(12):6618–6624.
24. Liu Y, Moënne-Loccoz P, Loehr TM, Ortiz de Montellano PR (1997) Heme oxygenase-1, intermediates in verdoheme formation and the requirement for reduction equivalents. *J Biol Chem* 272(11):6909–6917.
25. Zhang X, et al. (2003) Stereoselectivity of each of the three steps of the heme oxygenase reaction: Hemin to *meso*-hydroxyhemin, *meso*-hydroxyhemin to verdoheme, and verdoheme to biliverdin. *Biochemistry* 42(24):7418–7426.
26. Sano S, Sano T, Morishima I, Shiro Y, Maeda Y (1986) On the mechanism of the chemical and enzymic oxygenations of α-oxyprotohemin IX to Fe.biliverdin IX α. *Proc Natl Acad Sci USA* 83(3):531–535.
27. Sono M, Roach MP, Coulter ED, Dawson JH (1996) Heme-containing oxygenases. *Chem Rev* 96(7):2841–2888.
28. Knoot CJ, Purpero VM, Lipscomb JD (2015) Crystal structures of alkylperoxo and anhydride intermediates in an intradiol ring-cleaving dioxygenase. *Proc Natl Acad Sci USA* 112(2):388–393.
29. Ikeda-Saito M, Fujii H (2003) EPR characterization of the heme oxygenase reaction intermediates and its implication for the catalytic mechanism. *Paramagnetic Resonance of Metallobiomolecules (ACS Symposium)*, ed Tesler J (American Chemical Society, Washington, DC), Vol 858, pp 97–112.
30. Unno M, Matsui T, Ikeda-Saito M (2007) Structure and catalytic mechanism of heme oxygenase. *Nat Prod Rep* 24(3):553–570.
31. Schneider C, Pratt DA, Porter NA, Brash AR (2007) Control of oxygenation in lipoxygenase and cyclooxygenase catalysis. *Chem Biol* 14(5):473–488.
32. Takayama SJ, Ukpabi G, Murphy ME, Mauk AG (2011) Electronic properties of the highly ruffled heme bound to the heme degrading enzyme IsdI. *Proc Natl Acad Sci USA* 108(32):13071–13076.
33. Reniere ML, et al. (2010) The IsdG-family of haem oxygenases degrades haem to a novel chromophore. *Mol Microbiol* 75(6):1529–1538.
34. Sawaki Y, Foote CS (1979) Acyclic mechanism in the cleavage of benzils with alkaline hydrogen peroxide. *J Am Chem Soc* 101(21):6292–6296.
35. Ramette RW, Sandford RWJ (1965) Thermodynamics of iodine solubility and triiodide ion formation in water and in deuterium oxide. *J Am Chem Soc* 87(22):5001–5005.
36. Matera KM, et al. (1997) Histidine-132 does not stabilize a distal water ligand and is not an important residue for the enzyme activity in heme oxygenase-1. *Biochemistry* 36(16):4909–4915.
37. Maehly AC, Chance B (1954) The assay of catalases and peroxidases. *Methods Biochem Anal* 1:357–424.
38. Neya S, et al. (2010) Molecular insight into intrinsic heme distortion in ligand binding in hemoprotein. *Biochemistry* 49(27):5642–5650.
39. Hirota S, et al. (1994) Observation of a new oxygen-isotope-sensitive Raman band for oxyhemoproteins and its implications in heme pocket structures. *J Am Chem Soc* 116(23):10564–10570.
40. Takahashi S, et al. (1995) Oxygen-bound heme-heme oxygenase complex - Evidence for a highly bent structure of the coordinated oxygen. *J Am Chem Soc* 117(22):6002–6006.
41. Macdonald IDG, Sligar SG, Christian JF, Unno M, Champion PM (1999) Identification of the Fe-O-O bending mode in oxycytochrome P450cam by resonance Raman spectroscopy. *J Am Chem Soc* 121(2):376–380.